

Supersymmetric isospectral formalism for the calculation of near-zero energy states: application to the very weakly bound ^4He trimer excited state

Sudip Kumar Haldar^{1*}, Barnali Chakrabarti^{1,2}, Tapan Kumar Das³

¹*Department of Physics, Lady Brabourne College,
P-1/2 Suhrawardi Avenue, Kolkata 700017, India.*

²*Instituto de Física, Universidade de São Paulo, CP 66318, 05315-970, São Paulo, SP Brazil*

³*Department of Physics, University of Calcutta, 92 A P C Road, Kolkata 700009, India*

We propose a novel mathematical approach for the calculation of near-zero energy states by solving potentials which are isospectral with the original one. For any potential, families of strictly isospectral potentials (with very different shape) having desirable and adjustable features are generated by supersymmetric isospectral formalism. The near-zero energy Efimov state in the original potential is effectively trapped in the deep well of the isospectral family and facilitates more accurate calculation of the Efimov state. Application to the first excited state in ^4He trimer is presented.

PACS numbers: 03.75.Hh, 31.15.Ja, 03.65.Ge, 03.75.Nt

I. INTRODUCTION

It was proposed by Efimov in 1970 that if two spinless neutral bosons interact resonantly then the addition of a third identical particle leads to the appearance of an infinite number of bound three-body energy levels [1, 2]. This occurs simultaneously with the divergence of the s -wave scattering length (a_s), associated with appearance of an additional zero-energy two-body bound state. Hence highly exotic Efimov states appear when there is a zero or near-zero energy two-body bound state. For a long time there was no clear signature of Efimov states in any naturally occurring trimer system. Efimov states are not possible in atomic systems due to the long range Coulomb interaction, however it may exist in the system of spinless neutral atoms. Even though the Efimov effect was predicted four decades ago [1, 2], evidence of its existence in ultracold caesium and potassium trimers has been experimentally established only very recently [3]. However, these trimers are obtained by manipulating two-body forces through Feshbach resonances and are not naturally occurring. Therefore, it is of great interest to search for the Efimov effect in a naturally occurring trimer, like ^4He trimer. So far no experimental confirmation has been reported. The near-zero energy ($E_0 \sim 1$ mK) bound state (which is also the only bound state) of ^4He dimer opens the possibility of the existence of an Efimov-like state in ^4He trimer. Several authors remarked that the ^4He trimer may be the most promising candidate. Earlier theoretical calculations show that the trimer has a $L=0$ ground state at 126 mK and a near-zero energy excited state (~ 2 mK) [4–13]. The excited state has been claimed to be an Efimov state. A controversy arises from the fact that the number of Efimov states is highly sensitive to the binding energy of the dimer and even a very small

decrease of the strength of two-body interaction makes the system unbound. Strikingly, it also disappears when the two-body interaction strength is *increased*. However in contrast with theoretical investigations, no evidence of Efimov trimer has been found experimentally [14, 15]. In the experiments, ^4He trimer has been observed in its ground state only. No experimental evidence of the excited state has been reported so far.

In principle ^4He trimer may be considered as a very simple three-body system consisting of three identical bosons. But its theoretical treatment is quite difficult. First, the He-dimer potential is not uniquely known. Very small uncertainties in the dimer potential may lead to different conclusions. Secondly, the strong short-range interatomic repulsion in the He-He interaction causes large numerical errors. As ^4He systems are strongly correlated due to large ^4He - ^4He repulsion at short separation, the effect of interatomic correlation must be taken properly into account.

In the present communication, we revisit the problem using a correlated basis function known as potential harmonics (PH) basis which takes care of two-body correlations [16]. In order to include the effect of highly repulsive He-He core, we multiply the PH basis with a suitable short-range correlation function which reproduces the correct short-range behavior of the dimer wavefunction. Although this correlated PH basis (CPH basis) correctly reproduces the dimer and trimer properties, we could not find any Efimov like state in trimer with the actual dimer interaction [17]. We point out that the calculation of such a near-zero energy excited state in the shallow and extended trimer potential may involve severe numerical errors and we may miss it. Thus an alternative accurate procedure is desirable. Here, we apply the supersymmetric isospectral formalism for an accurate treatment. For any given potential, families of strictly isospectral potentials, *with very different shape* but having desirable and adjustable

*e-mail: sudip_cu@rediffmail.com

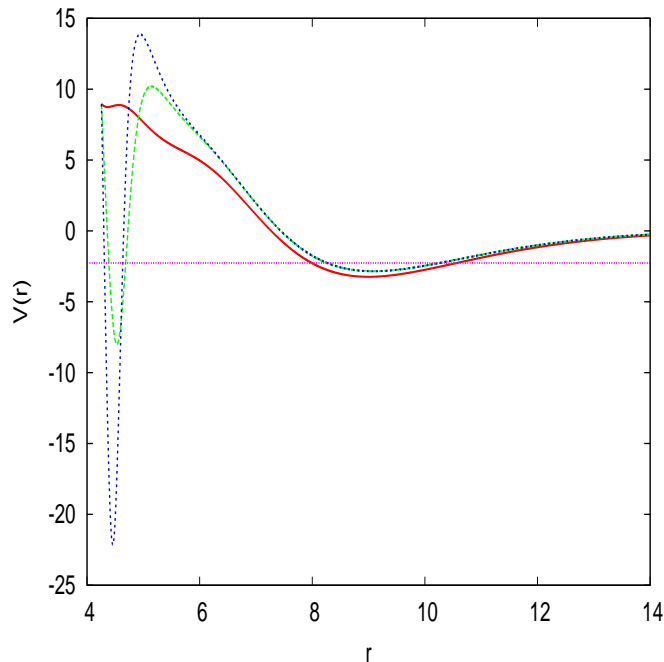


Fig. 1 (Color online) The effective potential $\omega_0(r)$ (red solid curve) and isospectral potentials $\hat{\omega}_0(r, \lambda)$ corresponding to two values of λ : $\lambda = 0.00005$ (green dashed curve) and $\lambda = 0.00002$ (blue dotted curve) for the ^4He trimer. All energies are in mK and r in a.u. The horizontal line indicates the energy of the first excited state in $\omega_0(r)$.

features are generated by supersymmetric isospectral formalism [18]. The near-zero energy bound state will be more effectively bound in the deep narrow well of the isospectral potential and will facilitate an easier and more accurate calculation of the near-zero energy excited state. Following the steps of supersymmetric quantum mechanics [18], for any given potential $\omega_0(r)$, one can construct a class of potentials $\hat{\omega}_0(r, \{\lambda\})$, where $\{\lambda\}$ represents a set of one or more continuously variable real parameters. The potential $\hat{\omega}_0$ is isospectral in the sense that ω_0 and $\hat{\omega}_0$ have identical spectrum, reflection and transmission coefficients. For simplicity we consider only one parameter (λ) family of isospectral potentials. We will see later that λ can take real values $-\infty < \lambda < -1$ and $0 < \lambda < \infty$. For $\lambda \rightarrow \infty$, one gets back the original potential. Although the set of isospectral potentials are strictly isospectral with the original potential, they have different shapes depending on the parameter λ [18]. In Fig. 1, we demonstrate how an original potential, $\omega_0(r)$ shown by the solid (red) curve, changes in the isospectral potential $\hat{\omega}_0(r, \lambda)$ for two values of the parameter λ , *viz.* $\lambda = 0.00005$ (green dashed curve) and $\lambda = 0.00002$ (blue dotted curve). We introduce this figure here for a qualitative understanding of the features of the isospectral potentials. A complete discussion of how such isospectral potentials are calculated will be presented in Sections II C and III. Although all three potentials produce identical energy spectrum, their shapes are seen

to be very different. The original potential $[\omega_0(r)]$ has a shallow and wide well with a short range repulsion. By contrast, both the isospectral potentials have a deep and narrow *attractive well* (NAW) at smaller r , while the long range part does not differ much from $\omega_0(r)$. One can also notice that as λ decreases, the narrow attractive well becomes deeper, while the intermediate barrier becomes higher. Hence, the near-zero energy (indicated in Fig. 1 by a horizontal line) excited state in $\omega_0(r)$ will be at the *same energy value* in the isospectral potentials, but now that state will lie *deep within the NAW*. Thus, while this state is weakly bound and spatially extended in the original potential, it will be strongly bound and well localized in the NAW of the isospectral potential, at the same energy. Clearly, computation of the wave function and its energy (equal to the energy of the first excited state in the original potential) will be easier. Furthermore, this state becomes more strongly bound, as λ decreases. In general, as λ decreases continuously from ∞ to 0, $\hat{\omega}_0$ starts developing a local minimum which shifts towards $r=0$ and becomes deeper and narrower. Consequently, a shallow potential transforms into one having a narrow and deep potential well near the origin in the isospectral potential. The surface barrier also becomes high. Such interesting properties of $\hat{\omega}_0$ can be useful to solve near-zero energy states. Such a state lies near the top of the original potential well and its wave function is spatially very extended, while the isospectral state lies well within the NAW. Hence the latter is strongly bound and well localized within the narrow well of V_1 . The parameter λ controls these features and a suitable optimum value can be chosen (see later).

Thus our approach consists of two steps. First, to apply a correlated quantum many-body theory for a highly correlated system like ^4He -trimer and second, to use the isospectral formalism for the accurate determination of the first excited state, whose energy is just a few mK.

The paper is organized as follows. In Section II, we present a brief review of the correlated potential harmonics expansion method, choice of potential and the isospectral formalism. Section III presents the results of our numerical calculation. Finally we draw our conclusions in Section IV.

II. THEORETICAL PROCEDURE

A. Correlated Potential harmonics expansion method

The Hamiltonian for a system of $(N + 1)$ atoms (each of mass m) and interacting via two-body potential has

the form

$$H = -\frac{\hbar^2}{2m} \sum_{i=1}^{N+1} \nabla_i^2 + \sum_{i>j=1}^{N+1} V(\vec{x}_i - \vec{x}_j) \quad (1)$$

where $V(\vec{x}_i - \vec{x}_j) = V(\vec{r}_{ij})$ is the He-He two-body potential described later. The relative motion in the standard Jacobi coordinates, $\{\vec{\zeta}_1, \dots, \vec{\zeta}_N\}$, is given by [16]

$$\left[-\frac{\hbar^2}{m} \sum_{i=1}^N \nabla_{\vec{\zeta}_i}^2 + V(\vec{\zeta}_1, \dots, \vec{\zeta}_N) - E \right] \Psi(\vec{\zeta}_1, \dots, \vec{\zeta}_N) = 0. \quad (2)$$

We decompose Ψ in Faddeev components

$$\Psi(\vec{x}) = \sum_{ij>i}^{N+1} \psi_{ij}(\vec{x}), \quad (3)$$

where $\psi_{ij}(\vec{x})$ is the two-body Faddeev component for the (ij) partition. In potential harmonics expansion method (PHEM), we expand (ij) -Faddeev component in the complete set of potential harmonics, $\{\mathcal{P}_{2K+l}^{lm}(\Omega_N^{(ij)})\}$, appropriate for (ij) -partition [16, 19]

$$\psi_{ij} = r^{-(\frac{3N-1}{2})} \sum_K \mathcal{P}_{2K+l}^{lm}(\Omega_N^{(ij)}) u_K^l(r). \quad (4)$$

PH basis is the subset of hyperspherical harmonics (HH), which is sufficient for the expansion of the two-body potential $V(\vec{r}_{ij})$, for the particular (ij) partition [16]. This PH function depends only on \vec{r}_{ij} and a global length r (called hyperradius). Hence Ψ in Eq. (3) includes only long range two-body correlations. $\Omega_N^{(ij)}$ represents the full set of hyperangles for the (ij) partition. The potential harmonics basis function for the (ij) -partition is given by [16]

$$P_{2K+l}^{lm}(\Omega_{ij}) = Y_{lm}(\omega_{ij})^{(N)} P_{2K+l}^{l,0}(\phi) \mathcal{Y}_0(D-3), \quad (5)$$

where $\phi = \cos^{-1}(r_{ij}/r)$, $Y_{lm}(\omega_{ij})$ is a spherical harmonic, ω_{ij} being the polar angles of \vec{r}_{ij} , $^{(N)} P_{2K+l}^{l,0}(\phi)$ is expressed in terms of Jacobi polynomials and \mathcal{Y}_0 is the lowest order hyperspherical harmonic in $(3N-3)$ dimensional hyperangular space (hence a constant) [19]. The basic assumption in Eq. (3) is that only two-body correlations are important and higher-body correlations are disregarded. Thus in the (ij) -Faddeev component, where only the (ij) -pair interacts, ψ_{ij} is independent of the coordinates of all particles except \vec{r}_{ij} . Hence we can freeze the contributions coming from $(N-1)$ remaining spectators. Thus the contribution to the orbital angular momentum and the grand orbital quantum number comes only from the interacting pair and the $3N$ dimensional Schrödinger equation reduces effectively to a four dimensional equation. The relevant set of quantum numbers, associated with the hyperangles, are three. These are orbital l , azimuthal m and grand orbital $2K+l$ for any N .

So far we have disregarded the effect of strong short range correlation in the PH basis. The He-He potential becomes suddenly very strongly repulsive below a certain value of interatomic separation. This causes a very strong short range two-body correlation in the many body wave function. We introduce this correlation function in the expansion basis and call it as CPH basis [20].

$$\left[\mathcal{P}_{2K+l}^{l,m}(\Omega_{(ij)}) \right]_{\text{correlated}} = Y_{lm}(\omega_{ij})^{(N)} P_{2K+l}^{l,0}(\phi) \mathcal{Y}_0(3N-3) \eta(r_{ij}), \quad (6)$$

where $\eta(r_{ij})$ is the short range correlation function. It is practically zero for very small r_{ij} ($r_{ij} < r_c$) where r_c is the size of the repulsive core. Its role is to enhance the speed of convergence of the expansion basis. We obtain $\eta(r_{ij})$ as the zero energy solution of (ij) -pair relative motion in the potential $V(r_{ij})$,

$$-\frac{\hbar^2}{m} \frac{1}{r_{ij}^2} \frac{d}{dr_{ij}} \left(r_{ij}^2 \frac{d\eta(r_{ij})}{dr_{ij}} \right) + V(r_{ij}) \eta(r_{ij}) = 0. \quad (7)$$

Replacing PH by CPH in Eq. (4) and taking projection of the Schrödinger equation on the PH basis of a particular partition, a set of coupled differential equation (CDE) is obtained [20]

$$\left[-\frac{\hbar^2}{m} \frac{d^2}{dr^2} + \frac{\hbar^2}{mr^2} \{ \mathcal{L}(\mathcal{L}+1) + 4K(K+\alpha+\beta+1) \} - E \right] U_{Kl}(r) + \sum_{K'} f_{Kl} V_{KK'}(r) f_{K'l} U_{K'l}(r) = 0, \quad (8)$$

where $\mathcal{L} = l + \frac{3N-3}{2}$, $\alpha = \frac{3N-5}{2}$, $\beta = l + \frac{1}{2}$ and f_{Kl} is a constant representing the overlap of a PH corresponding to a particular partition with the sum of PHs of all partitions [20]. K is the hyperangular momentum quantum number. The correlated potential matrix element $V_{KK'}(r)$ is now given by [20]

$$V_{KK'}(r) = (h_K^{\alpha\beta} h_{K'}^{\alpha\beta})^{-\frac{1}{2}} \int_{-1}^{+1} P_K^{\alpha\beta}(z) V \left(r \sqrt{\frac{1+z}{2}} \right) P_{K'}^{\alpha\beta}(z) \eta \left(r \sqrt{\frac{1+z}{2}} \right) W_l(z) dz. \quad (9)$$

Here $h_K^{\alpha\beta}$ and $W_l(z)$ are respectively the norm and weight function of the Jacobi polynomial $P_K^{\alpha\beta}$ [16].

B. Choice of He-He potential

For a realistic calculation, one needs an accurate He-He interaction potential. Several sophisticated He-He potentials have been proposed [21]. Among these, the commonly used ones are: Tang, Tonnies and Yiu (TTY) [22],

LM2M2 [23], and HFD-HE2 [24] potentials. These potentials reproduce all known two-body He-He data. In the present work, we select the more popular and sophisticated TTY potential. This potential has the form [11, 22]

$$V(x) = A[V_{ex}(x) + V_{disp}(x)], \quad (10)$$

where x represents the interparticle distance. The part V_{ex} has the form $V_{ex}(x) = Dx^p e^{-2\gamma x}$ with $p = \frac{7}{2\gamma} - 1$. The other part V_{disp} is given as $V_{disp}(x) = -\sum_{n=3}^{12} C_{2n} f_{2n}(x) x^{-2n}$. The coefficients C_{2n} are calculated using the recurrence relation $C_{2n} = \left(\frac{C_{2n-2}}{C_{2n-4}}\right)^3 C_{2n-6}$; $C_6 = 1.461$, $C_8 = 14.11$, $C_{10} = 183.5$, $A = 315766.2067 K$, $D = 7.449$ and $\gamma = 1.3443 (a.u.)^{-1}$. The function f_{2n} is given by $f_{2n}(x) = 1 - e^{-bx} \sum_{k=0}^{2n} \frac{(bx)^k}{k!}$ with $b(x) = 2\gamma - \frac{p}{x}$.

For our numerical solution, the set of CDEs [Eq. (8)] is solved by hyperspherical adiabatic approximation (HAA) [25]. In HAA, one assumes that the hyperradial motion is slow compared to the hyperangular motion. The effective potential for the hyperradial motion (obtained by diagonalizing the potential matrix together with the diagonal hypercentrifugal repulsion for a fixed value of r) is obtained as a parametric function of r . We choose the lowest eigenpotential ($\omega_0(r)$) as the effective potential. Thus in HAA, energy and wavefunction are obtained approximately by solving a single uncoupled differential equation

$$\left[-\frac{\hbar^2}{m} \frac{d^2}{dr^2} + \omega_0(r) - E \right] \zeta_0(r) = 0, \quad (11)$$

subject to appropriate boundary conditions on $\zeta_0(r)$. The principal advantage of the present method is two-fold. Firstly, the CPH basis set correctly takes care of the effect of strong short range correlation produced by the He-He interaction. Secondly, the use of HAA basically reduces the multidimensional problem to an effective one dimensional problem introducing the effective potential. The effective potential ($\omega_0(r)$) gives a clear qualitative as well as quantitative picture. For our numerical calculation we investigate the $l = 0$ state and truncate the CPH basis to a maximum value $K = K_{max}$, requiring proper convergence.

The ground state properties of ^4He dimer is obtained as a numerical solution of two-body Schrödinger equation by Runge-Kutta algorithm. The dimer energy ϵ_d using TTY potential, as well as the results from other references are presented in Table I.

Although in our earlier calculation [17] we reported the dimer and trimer ground state properties, we include them here for completeness of the discussion. Calculated rms value of r_{ij} is 98.596 a.u. The extremely small

TABLE I: The ^4He -dimer energy using TTY potential.

Expt.	$\epsilon_d(\text{mK})$
$1.1_{-0.2}^{+0.3}$	present method -1.254
mK	DMC [23] -1.243
[27]	Other [11] -1.309
	Other [8] -1.313

binding energy of the dimer and the large spatial extension of the ground state wave function imply that the ground state of helium dimer is very loosely bound. The trimer ground state energy, as well as the results obtained in earlier investigations by other authors are presented in Table II for different potentials. The r.m.s. value of hyperradius is 21.389 a.u. Thus our correlated PH basis successfully reproduces the energy values which are in very close agreement with other sophisticated calculations [5–8, 11, 26–29].

TABLE II: The absolute value of ^4He -trimer ground state energy (in units of mK) obtained by different methods.

Potential	PHEM	variational	Faddeev	Adiabatic	DMC
TTY	125.51	126.40[24]	126.4 [7]	-	125.46 [25]
LM2M2	126.37	126.40 [25]	126.4 [7]	125.2 [6]	
HFDHE2	120.28		117.1 [7]	98.1 [5]	

Although we have done detailed calculation of ^4He trimer ground state energy, we failed to obtain any trimer excited state with this choice of two-body interaction. Very recently we have analyzed in details the behavior of ^4He trimer excited states as a function of pairwise interaction

$$V_{He-He} = \delta V_{TTY} \quad (12)$$

where δ controls the strength of two-body interaction. $\delta = 1$ is the physical value of the dimer interaction and $\delta = 0$ corresponds to free particle limit when neither two-body nor three-body bound states appear. We found that by increasing δ from a small value, the trimer starts to support an excited state at $\delta = 0.978$ [17]. Binding energy of the excited state gradually increases with increase in δ , attains its maximum value at $\delta = 0.984$, then it decreases gradually and disappears which indicates dissociation to trimer fragments as a dimer and monomer. Thus the disappearance of the first excited state due to both increasing and decreasing δ clearly show that the state is an Efimov state. But the value of δ for which this happens, does not correspond to the actual physical dimer interaction ($\delta = 1$). The Efimov property of other excited states are also discussed in our earlier study [17]. However we did not claim that the

trimer excited state does not exist at all, as there is a large body of work in this direction [4–13]. So this is still an ongoing issue as there is considerable controversy in the earlier discussions found in Refs [4–13]. Thus our earlier work could not resolve the problem. It may be the limitation of our basis set which is unable to produce such an elusive state. So it needs further study.

C. Isospectral formalism

For an accurate determination of the elusive near-zero energy excited state, we use the supersymmetric isospectral formalism mentioned earlier. Note that this state lies near the top of the potential well $\omega_0(r)$ and is very extended spatially. Consequently, a convergent calculation requires a very large number of hyperspherical partial waves (corresponding to very large K_{max}). On the other hand, the trimer ground state lies near the bottom of this well, is well bound and localized; it therefore converges relatively easily. Now the isospectral potential $\hat{\omega}_0(\lambda, r)$ with sufficiently small positive λ will have a deep well near the origin, followed by a high barrier (see below). The near-zero energy state sought after is now strongly trapped within this narrow well, *i.e.* it is sharply localized. Hence its convergence is achieved easily enough. The isospectral potential is obtained in terms of the trimer ground state wave function (see below), which by the above argument is determined with a fair degree of confidence and it offers easier calculation of the excited state.

Since isospectral formalism is not a common topic, we briefly explain how an isospectral potential is obtained for a given potential [18]. For the given potential $\omega_0(r)$ having a normalized ground state $\zeta_0(r)$ with energy E_0 , [see Eq. (11)], a superpotential $W(r)$ is defined as

$$W(r) = -\frac{\hbar}{\sqrt{m}} \frac{\zeta_0'(r)}{\zeta_0(r)}. \quad (13)$$

Then it can easily be seen that

$$\omega_0(r) - E_0 = W^2(r) - \frac{\hbar}{\sqrt{m}} W'(r), \quad (14)$$

and one can define a supersymmetric partner potential $\omega^{(2)}(r)$ through

$$\omega^{(2)}(r) - E_0 = W^2(r) + \frac{\hbar}{\sqrt{m}} W'(r), \quad (15)$$

such that $\omega_0(r)$ and its partner have the same energy spectra, except that the ground state of $\omega_0(r)$ is absent in the spectrum of its partner [18].

Now, for the given partner potential $\omega^{(2)}(r)$, Eq. (15) can be considered as a non-linear differential equation

satisfied by the unknown function $W(r)$ (called Riccati equation). With this $W(r)$, we can get back $\omega_0(r)$, using Eq. (14). But solution of the non-linear Eq. (15) is not unique. For simplicity, we use the units in which $\frac{\hbar^2}{m} = 1$. Then the most general solution is [18]

$$\hat{W}(r, \lambda) = W(r) + \frac{d}{dr} \ln |I_0(r) + \lambda|, \quad (16)$$

where λ is an integration constant and $\hat{W}(r, \lambda)$ is a function of r , parametrically dependent on λ . $I_0(r)$ is given by

$$I_0(r) = \int_0^r [\zeta_0(r')]^2 dr'. \quad (17)$$

Then the family of potentials $\hat{\omega}_0(r, \lambda)$ given by

$$\begin{aligned} \hat{\omega}_0(r, \lambda) - E_0 &= \hat{W}^2(r, \lambda) - \hat{W}'(r, \lambda) \\ \hat{\omega}_0(r, \lambda) &= \omega_0(r) - 2 \frac{d^2}{dr^2} \ln |I_0(r) + \lambda| \end{aligned} \quad (18)$$

for all allowed values of λ (see below), has the *same partner* $\omega^{(2)}(r)$. Hence the family of potentials given by Eq. (18) all have identical spectrum. Since $\zeta_0(r)$ is normalized, $0 \leq I_0(r) \leq 1$. Hence from Eq. (16), one notices that the interval $-1 \leq \lambda \leq 0$ is not allowed. For all other values of λ , $\hat{\omega}_0(r, \lambda)$ is strictly isospectral with $\omega_0(r)$ [18, 30]. For $\lambda = \infty$, $\hat{\omega}_0(r, \lambda)$ becomes $\omega_0(r)$. For small positive values of λ , the isospectral potential $\hat{\omega}_0(r, \lambda)$ develops an attractive well near the origin. As $\lambda \rightarrow 0$, this well becomes deeper followed by a high barrier, before the shallower part. Note that the ground state of $\omega_0(r)$, *viz.* $\zeta_0(r)$, is necessary to calculate the family of isospectral potentials. In the present study the ground state of $\omega_0(r)$ is fairly accurately calculated. We will see in the next section that different eigen states are transformed differently. Therefore this transformation cannot be considered as a generalized rotation in the Hilbert space. Thus the transformation from the original Hamiltonian to the isospectral Hamiltonian is different from a standard unitary transformation, even though the entire energy spectrum is preserved.

III. RESULTS AND DISCUSSIONS

First we calculate the lowest effective potential $\omega_0(r)$ in the hyperradial space by hyperspherical adiabatic approximation (HAA) as stated in Sec. IIB. To calculate the energy E and wave function $\zeta_0(r)$ of the original potential we solve the single uncoupled equation, Eq. (11), with appropriate boundary conditions. As stated earlier, although our calculated ground state energy E_0 and wave function are in good agreement with other calculations, we fail to get the first excited state in such a shallow potential. Here the isospectral formalism will be an effective technique to calculate several isospectral potentials of gradually varying shape,

which will facilitate easier calculation of the very weakly bound state. We calculate $I_0(r)$ from Eq. (17) and then the isospectral potential for a specific value of λ is calculated from Eq. (18).

In Fig. 1, the effective potential $\omega_0(r)$ calculated by the CPH method is shown as a continuous (red) curve. This has a soft repulsion at smaller r , followed by a shallow minimum which supports the ground state at 125.51 mK. As stated earlier, we fail to get the first excited state in this effective potential, by our numerical calculation. Next we calculate the isospectral potential $\hat{\omega}_0(r, \lambda)$, for chosen values of λ . We checked that for large values of λ , calculated $\hat{\omega}_0(r, \lambda)$ is practically indistinguishable from $\omega_0(r)$. For small values of λ , the isospectral potential develops a deep and narrow well near the origin (left side well, LSW) with a barrier (intermediate barrier, IB) separating it from the shallow well (right side well, RSW). As λ decreases towards zero, LSW becomes deeper, narrower and closer to the origin and at the same time, IB becomes higher.

TABLE III: Parameters of the original and the isospectral potentials. $\lambda = \infty$ corresponds to the original potential. LSW, IB and RSW respectively represent the left side well, the intermediate barrier and the right side well. Position values are in a.u. and energies are in mK.

λ	LSW		IB		RSW	
	r_{min}^{left}	ω_{min}^{left}	r_{max}	ω_{max}	r_{min}^{right}	ω_{min}^{right}
∞					8.999	-3.238
0.00010	4.607	-1.897	5.327	8.333	9.087	-2.848
0.00005	4.527	-8.119	5.137	10.23	9.087	-2.847
0.00002	4.457	-22.133	4.943	13.874	9.085	-2.846
0.00001	4.417	-40.254	4.817	18.019	9.085	-2.846

In Table III, we present numerical values of the parameters of the original (corresponding to $\lambda = \infty$) and isospectral potentials $\hat{\omega}_0(r, \lambda)$ for $\lambda = 0.00010, 0.00005, 0.00002$ and 0.00001 . For each isospectral potential, we give values of the position (r_{min}^{left}) and value (ω_{min}^{left}) of the minimum of LSW, position (r_{max}) and value (ω_{max}) of the maximum of IB, and position (r_{min}^{right}) and value (ω_{min}^{right}) of the minimum of RSW. We have checked by numerical calculation that the energy of both the ground and the first excited state remains independent of the choice of λ , as theory predicts. However, very small values of λ are not convenient for numerical calculation of the energy of the excited state, as numerical errors creep in, due to extreme narrowness of the LSW, in which the excited state resides. Thus a judicious choice of the value of λ is necessary. By careful investigations for different values of λ , we find that the range $0.00002 - 0.00005$ for the value of λ is optimum for minimizing errors. As two typical cases demonstrating the behavior of isospectral

potentials, we plot $\hat{\omega}_0(r, \lambda)$ for $\lambda = 0.00002$ (blue, dotted curve) and $\lambda = 0.00005$ (green, dashed curve) in Fig. 1. The very weakly bound first excited state in the original shallow potential $\omega_0(r)$ now becomes strongly bound within the deep and narrow LSW of $\hat{\omega}_0(r, \lambda)$. The deep well and the adjacent high barrier strongly localizes this state in the isospectral potential. We solve Eq. (11), with $\omega_0(r)$ replaced by $\hat{\omega}_0(r, \lambda)$, subject to appropriate boundary conditions to calculate the energy of the first excited state. Following this isospectral technique, we do indeed get a bound first excited state. We also verified that its energy is the same, within estimated numerical errors, for values of λ lying within the chosen range. The binding energy of the first excited state of trimer is thus found to be 2.270 mK. We present this result, together with results of other sophisticated calculations reported so far in Table IV.

TABLE IV: Results for energy of the first excited state of ${}^4\text{He}$ -trimer (in units of mK) obtained by different methods.

Reference	Energy
Ref [11]	-2.282
Ref [7]	-2.280
Ref [8]	-2.277
Present Method	-2.270

Here we remark that the isospectral formalism is an efficient tool to calculate near-zero energy states in shallow potential which supports at least one bound state. In the supersymmetric isospectral formalism, one can in principle calculate the energy value as well as the wave function. In our earlier calculation of the resonances of halo nuclei, we used the wave function of the isospectral potential. We calculated the probability of the system to be trapped in the well-barrier combination which facilitates the accurate determination of resonance energy [30, 31]. We have observed that the resonance energy is independent of λ . However in the present application to calculate the bound state wave function in the isospectral potentials and to calculate other physical observables we should take a different approach. From Fig. 1, we see that decreasing λ gradually keeps the long-range part of the isospectral potentials almost unchanged whereas the short-range part has a drastic change. Naturally the wave functions of the isospectral family are now λ dependent and obviously the calculated physical observables [e.g. average radius of the system] will be λ dependent. In the SUSY isospectral formalism [18], it is possible to calculate the wave function of the original potential $\omega_0(r)$ from the wave functions of the isospectral potential $\hat{\omega}_0(r, \lambda)$. The ground state $\hat{\zeta}_0(r, \lambda)$ and the first excited state $\hat{\zeta}_1(r, \lambda)$ of the isospectral potential $\hat{\omega}_0(r, \lambda)$ corresponding to the energies E_0 and E_1 respectively are

related to the ground state $\zeta_0(r)$ and the first excited state $\zeta_1(r)$ of the original potential $\omega_0(r)$ by [18]

$$\hat{\zeta}_0(r, \lambda) = \frac{\zeta_0(r)}{I_0 + \lambda} \quad (19)$$

and

$$\hat{\zeta}_1(r, \lambda) = (E_1 - E_0)\zeta_1 + \hat{\zeta}_0\mathcal{W}(\zeta_0, \zeta_1) \quad (20)$$

where $\mathcal{W}(\zeta_0, \zeta_1) = \zeta_0\zeta_1' - \zeta_1\zeta_0'$ is the Wronskian and $\zeta_0(r)$ and $\zeta_1(r)$ are well-behaved functions. We can calculate the ground state wave function $\hat{\zeta}_0(r, \lambda)$ of the isospectral potential $\hat{\omega}_0(r, \lambda)$ from the original ground state wave function $\zeta_0(r)$ (which is known as we calculated it to construct the family of isospectral potentials) using Eq. (19). Alternatively we can obtain $\hat{\zeta}_0(r, \lambda)$ directly by solving for the isospectral potential $\hat{\omega}_0(r, \lambda)$. Also we can obtain $\hat{\zeta}_1(r, \lambda)$ by solving for the isospectral potential $\hat{\omega}_0(r, \lambda)$ with energy E_1 . Thus Eq. (20) is a first order differential equation in $\zeta_1(r)$ and we can solve it subject to proper boundary conditions $\zeta_1(0) = 0$ and $\zeta_1'(0) \neq 0$ to obtain $\zeta_1(r)$. With these wave functions we can calculate any physical properties of the system and this time they will be independent of the λ . However usually in the SUSY isospectral formalism, people are interested only in the bound state energy and in this paper we are also interested only in the energy of the elusive first excited state.

Next we discuss in detail about the choice of λ parameter. As in our earlier works [31–33], we observe that the energy is independent of the parameter λ . But making λ too small, may create large numerical error in the numerically calculated wave function $\hat{\zeta}_1(r, \lambda)$, as the well becomes extremely narrow and very deep. Then the wave function changes very rapidly over a very small interval. Clearly its derivatives are inaccurate, which in turn affects the accuracy of the wave function at the next mesh point. The errors accumulate. As we solve the isospectral potential numerically, large numerical error will result for very small λ . This may mask the overall accuracy. Thus the accuracy of the results are very crucially dependent on the choice of λ . There is no prescribed rule to choose λ . It is in general chosen by trial. One can choose finer mesh interval within the LSW for a small λ . But the cumulative error at successive mesh point, increases as the total number of mesh points increases. Using the error estimate of the integration

procedure (we use Runge-Kutta algorithm) we optimize the values of λ and mesh interval to minimize the error. In our earlier calculations [31, 32] for 2_1^+ state of ${}^6\text{He}$, the shallowness of the effective potential is removed for $\lambda = 10$, whereas $\lambda = 0.1$ was required for 2_2^+ state of the same system to get the expected behavior of the isospectral potential. Thus the optimum choice of λ depends on the choice of the system and its state.

Now in principle the ground state energy can also be recalculated using the isospectral potentials, in which the ground state of the original potential now lies in the very deep well of the isospectrals. But, when we solve the isospectral potential numerically, large error may creep due to the extreme narrowness of the well, as discussed above. Thus when we use the isospectral formalism for the real many-body problems, ground state energy is more accurate when determined by the original potential and the excited states and resonance states are more accurate when we solve the isospectral potentials.

IV. CONCLUSIONS

In conclusion, we remark that the isospectral potential with a judiciously chosen value of λ can be very useful for an accurate calculation of near-zero energy states in a shallow potential and also the resonance states of halo and highly unstable systems. The present application to the very weakly bound and highly elusive first excited state in ${}^4\text{He}$ trimer demonstrates the novelty and practical utility of this technique.

This work has been partially supported by FAPESP (Brazil), CNPq (Brazil), Department of Science and Technology (DST, India) and Department of Atomic Energy (DAE, India). B.C. wishes to thank FAPESP (Brazil) for providing financial assistance for her visit to the Universidade de São Paulo, Brazil, where part of this work was done. SKH wishes to thank the Council of Scientific and Industrial Research (CSIR), India for a Junior Research Fellowship. T.K.D. acknowledges the University Grants Commission (UGC, India) for the Emeritus Fellowship.

[1] V. Efimov, Phys. Lett. B **33**, 563 (1970).
 [2] V. Efimov, Nucl. Phys. A **210**, 157 (1973).
 [3] T. Kraemar *et al.*, Nature **440**, 315 (2006); S. Knoop *et al.*, Nature Phys. Lett. **5**, 227 (2009); M. Zaccanti *et al.*, Nature Phys. **5**, 586 (2009).
 [4] T. Cornelius and W. Glöckle, J. Chem. Phys. **85**, 3906

(1986).
 [5] B. D. Esry, C. D. Lin, and C. H. Greene, Phys. Rev. A **54**, 394 (1996).
 [6] E. Nielsen, D. V. Fedorov and A. S. Jensen, J. Phys. B **31**, 4085 (1998)
 [7] V. Roudnev and S. Yakovlev, Chem. Phys. Lett. **328**, 97

- (2000).
- [8] P. Barletta and A. Kievsky, Phys. Rev. A **64**, 042514 (2001).
- [9] W. Sandhas, E. A. Kolganova, Y. K. Ho and A. K. Motovilov, Few-Body Syst. **34**, 137 (2004).
- [10] T. González-Lezana *et al.*, Phys. Rev. Lett. **82**, 1648 (1999).
- [11] A. K. Motovilov, W. Sandhas, S. A. Sofianos and E. A. Kolganova, Eur. Phys. J. D **13**, 33 (2001).
- [12] H. Suno and B. D. Esry, Phys. Rev. A **78**, 062701 (2008).
- [13] E. Braaten, H. W. Hammer, D. Kang, and L. Platter, Phys. Rev. A **78**, 043605 (2008).
- [14] W. Schöllkopf and J. P. Toennies, Science **266**, 1345 (1994).
- [15] R. Brühl *et al.*, Phys. Rev. Lett. **95**, 063002 (2005).
- [16] M. Fabre de la Ripelle, Ann. Phys. (N.Y.) **147**, 281 (1983).
- [17] T. K. Das, B. Chakrabarti and S. Canuto, J. Chem. Phys. **134**, 164106 (2011).
- [18] F. Cooper, A. Khare and U. Sukhatme, Phys. Rep. **251**, 267 (1995).
- [19] T. K. Das and B. Chakrabarti, Phys. Rev. A **70**, 063601 (2004).
- [20] T. K. Das *et al.*, Phys. Lett. A **373**, 258 (2009).
- [21] A. R. Janjen and R. A. Aziz, J. Chem. Phys. **103**, 9626 (1995).
- [22] K. T. Tang, J. P. Toennies, C. L. Yiu, Phys. Rev. Lett. **74**, 1546 (1995).
- [23] R. A. Aziz and M. J. Slaman, J. Chem. Phys. **94**, 8047 (1991).
- [24] R. A. Aziz, V. P. S. Nain, J. S. Carley, W. L. Taylor, and G. T. McConville, J. Chem. Phys. **70**, 4330 (1979).
- [25] T. K. Das, H. T. Coelho and M. Fabre de la Ripelle, Phys. Rev. C **26**, 2281 (1982).
- [26] M. Lewerenz, J. Chem. Phys. **106**, 4596 (1997).
- [27] D. Bressanini *et al.* J. Chem. Phys. **112**, 717 (2000).
- [28] D. Blume and C. H. Greene, J. Chem. Phys. **112**, 8053 (2000).
- [29] R. Grisenti, W. Schöllkopf and J. P. Toennies, Phys. Rev. Lett. **85**, 2284 (2000).
- [30] T. K. Das and B. Chakrabarti, Phys. Letts A **288**, 4 (2001).
- [31] S. K. Dutta, T. K. Das, M. A. Khan and B. Chakrabarti Few-Body Systems **35**, 33 (2004).
- [32] S. K. Dutta, T. K. Das, M. A. Khan and B. Chakrabarti, J. Phys. G: Nucl. Part. Phys. **29**, 2411 (2003).
- [33] B. Chakrabarti, Proceedings of Conference on 'Non-Hermitian Hamiltonian in Quantum Physics', BARC, India, June 13 - 16, 2009 [Pramana, Journal of Physics, **73**, 405 (2009)].